

# A Novel Dual Material Bionic Flexible Logo Antenna with EBG Structure

Daming Lin<sup>1</sup>, Encheng Wang<sup>2, \*</sup>, Jie Wang<sup>3</sup>, Wen Zhang<sup>4</sup>, and Hao Zhang<sup>4</sup>

**Abstract**—Based on the principle of bionics, this paper combines the design of flexible bionic antenna with Chinese culture and proposes a dual-material bionic antenna with Electromagnetic Band Gap (EBG) structure. The antenna uses a polyimide flexible substrate. Radiation patch of this antenna is shaped like a “pear flower”, and the “CHINA” shaped slot is etched on the ground to form a Logo mark. In order to reduce the impact of antenna radiation on human body, the introduction of an EBG structure made of Polydimethylsiloxane (PDMS) material makes the front-to-back ratio of the antenna radiation significantly increased. The antenna was bent in different ways and placed on human body model for simulation and testing. The results showed that the antenna achieved an impedance bandwidth of 18.8% (2.22–2.46 GHz), peak gain of 4.02 dBi, and the antenna was low sensitive to deformation, which makes it suitable for modern flexible electronic equipment. From the perspective of bionics, the antenna has good radiation and wearable type, and the beautiful pattern improves the viewing ability of the antenna and people’s willingness to wear the wearable antenna, which provides a new design idea for the future design of wearable devices.

## 1. INTRODUCTION

Colorful flowers with different shapes are gifts from nature. For thousands of years, people have researched and used the forms, structures, functions and working principles of natural creatures to invent and create brand-new technologies and tools. The bionic antenna is a new kind of antenna with specific functions produced by combining bionics and antenna design. Bionic antennas can be divided into functional bionic antennas, morphological bionic antennas, color bionic antennas, and structural bionic antennas. In [1], a bionic ultra-wideband antenna was proposed based on insect antennae, which effectively reduced the antenna radar cross section. In [2], a bionic Yagi antenna based on plant leaves was proposed, which is suitable for applications in guidance, detection, and radar.

With the continuous improvement of the level of technology, various wearable devices continue to emerge and are more and more widely used in military detection, tracking and positioning, medical health, leisure and entertainment. The popularity of wearable devices has greatly increased the demand for flexible antennas, and the performance requirements have become more stringent. In the design of flexible antenna, appearance, comfort, flexibility, and the influence of antenna on human body are particularly important [3–6]. [7] designed a dual-band antenna for WLAN and WiMAX bands. Utilizing conductive oxide materials, the transparent properties were achieved, which greatly reduced the space constraints for antenna usage. [8] designed a transparent four-element MIMO antenna to achieve 85% transparency, applied in 5G mm-wave spectrum, and has broad development prospects in future smart devices.

---

*Received 15 November 2021, Accepted 5 March 2022, Scheduled 14 March 2022*

\* Corresponding author: Encheng Wang (wefyx@163.com).

<sup>1</sup> Research Institute of Highway, Ministry of Transport, Beijing 100088, China. <sup>2</sup> Information Engineering College of North China University of Technology, 10044, China. <sup>3</sup> College of Civil Engineering of North China University of Technology, 10044, China.

<sup>4</sup> College of Electronic and Information Engineering of Shandong University of Science and Technology, China.

In this paper, the principle of bionics is used to the design of flexible antenna, and the design can improve the aesthetics of the antenna on the premise of ensuring the performance of the antenna. By slotting on the ground, a logo mark is designed to further reduce the reflection coefficient and improve the antenna matching [9–11]. In order to reduce the antenna’s backward radiation, an EBG structure [12] is introduced to make the main lobe more concentrated and increase the antenna gain. Wearing wear will not significantly reduce the performance of the antenna for its small size and easy conformation. The antenna design details are presented in Section 2. Section 3 presents the EBG structure, and the performance of the antenna with EBG structure is simulated and measured. Finally, Section 4 simulates the application of the antenna and tests the performance of the antenna when it is structurally deformed and placed on the human body.

## 2. ANTENNA DESIGN

Pear flower is Rosaceae Pyrus genus, the flowers of pear trees, as shown in Figure 1(a). In this paper, the structure of a bionic pear flower shaped flexible antenna is shown in Figure 1(b). The antenna uses organic polymer material polyimide (PI) as the dielectric substrate, which has the characteristics of good mechanical properties, high temperature resistance, and easy bending. Relative permittivity and loss tangent of PI substrate are 3.1 and 0.0025. The antenna radiation patch is in the shape of a pear flower, and the ground plate on the back is etched with a “CHINA” shaped slot. The overall size of the antenna is 44.2 mm × 25.9 mm × 0.2 mm. Based on monopole antenna design theory, the initial antenna frequency corresponds to the wavelength which is calculated as follows:

$$\lambda_e = \frac{c}{f\sqrt{\frac{\epsilon_r + 1}{2}}} \quad (1)$$

where  $c$  is the speed of light in vacuum, and  $\epsilon_r$  is the dielectric constant of substrate. The detailed dimensions of the antenna are shown in Table 1.

The design process of the proposed bionic pear flower shaped antenna with the “CHINA” logo is described in Figure 2. According to [3], a 50Ω impedance-matched rectangular patch monopole Ant.1 is designed, and the antenna size is 127 mm × 87 mm × 0.23 mm. For reducing the size of the antenna, Ant.2 is proposed by loading a circular patch on the top of the rectangular antenna. Compared with

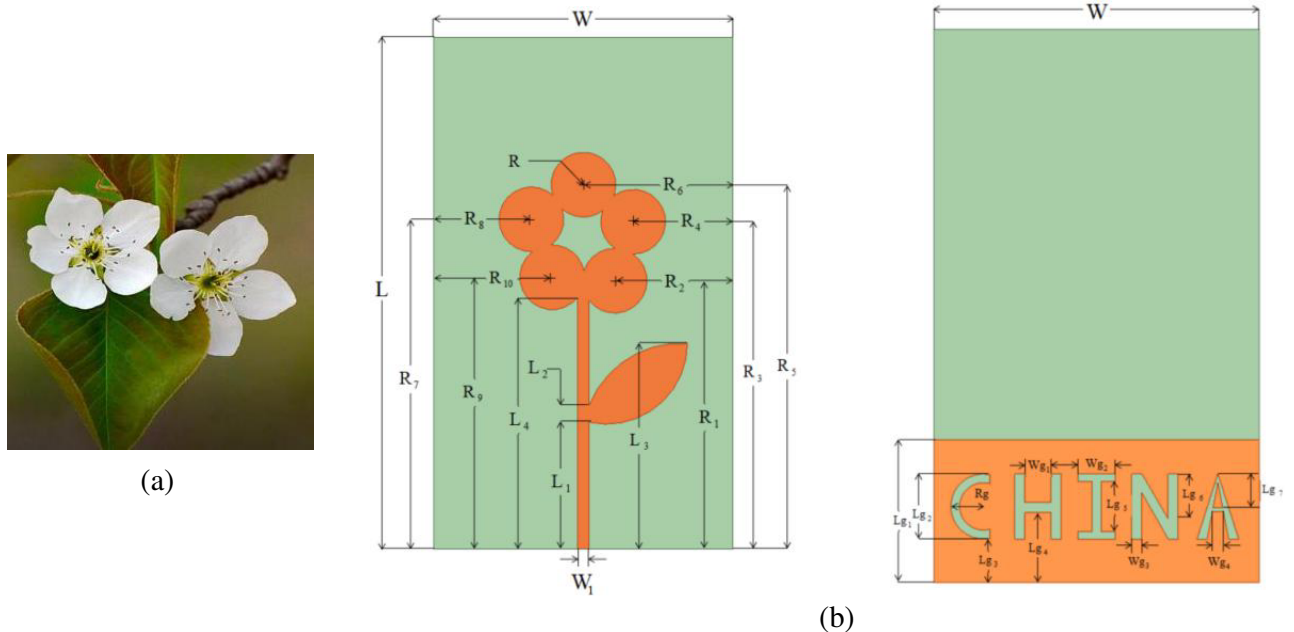


**Figure 1.** (a) Pear flowers in nature; (b) Bionic pear-shaped antenna structure diagram.

**Table 1.** Dimension of the proposed antenna of Fig. 1(b).

Parameter	Size (mm)	Parameter	Size (mm)	Parameter	Size (mm)
$L$	44.2	$R_4$	8.7	$L_{g4}$	5.6
$W$	25.9	$R_5$	31.5	$L_{g5}$	4
$L_1$	11	$R_6$	13	$L_{g6}$	3.7
$L_2$	1.4	$R_7$	28.5	$L_{g7}$	2.7
$L_3$	17.8	$R_8$	8.5	$W_{g1}$	2.1
$L_4$	21.8	$R_9$	23.5	$W_{g2}$	3
$R$	2.8	$R_{10}$	10.25	$W_{g3}$	0.8
$R_1$	23.2	$L_{g1}$	11.4	$W_{g4}$	0.8
$R_2$	10.3	$L_{g2}$	5.1	$W_1$	1
$R_3$	28.3	$L_{g3}$	3.5	$R_g$	2.6

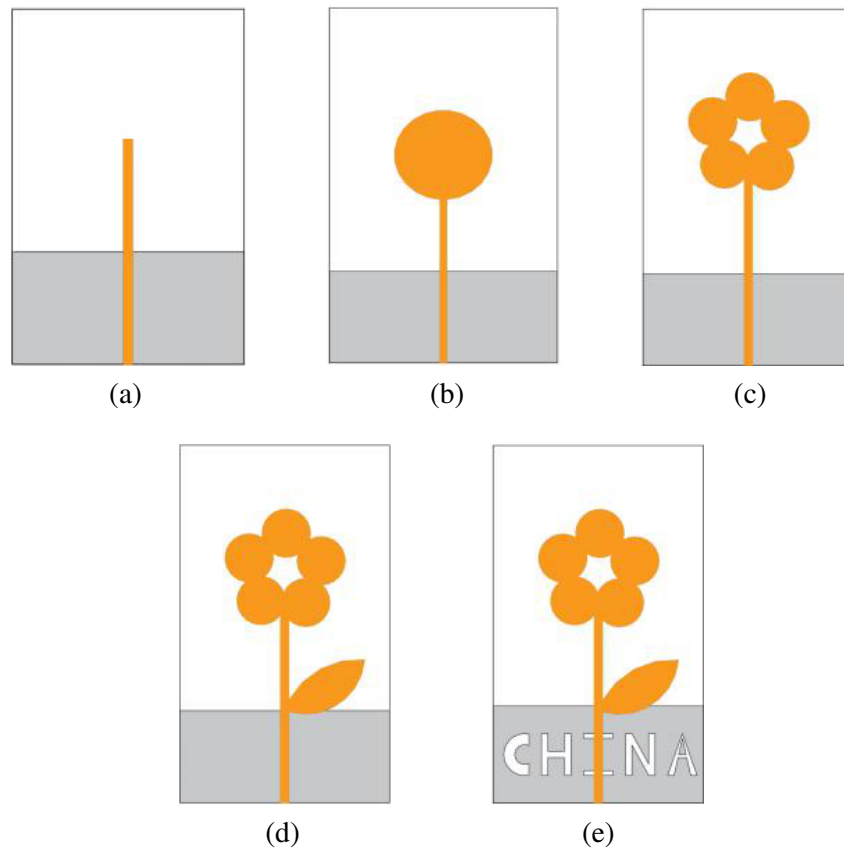


**Figure 2.** The design process of the bionic pear flowers shaped antenna. (a) Ant.1, (b) Ant.2, (c) Ant.3, (d) Ant.4, (e) Ant.5.

traditional loaded rectangular patch, this method can reduce the size of the antenna to achieve better impedance matching effect, thereby improving the performance of the antenna. By imitating the shape of pear flower in nature, a bionic pear flower Ant.3 is proposed. On the basis of Ant.3, a leaf-shaped patch is loaded to make the antenna more beautiful and more in line with the design requirements of the wearable antenna. Finally, a slot is etched on the antenna ground plate to form a “CHINA” logo

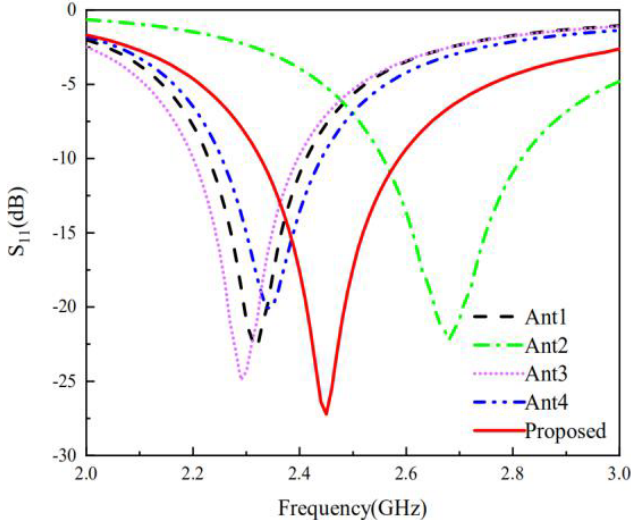


**Figure 3.** Comparison curve of reflection coefficient of five antennas.

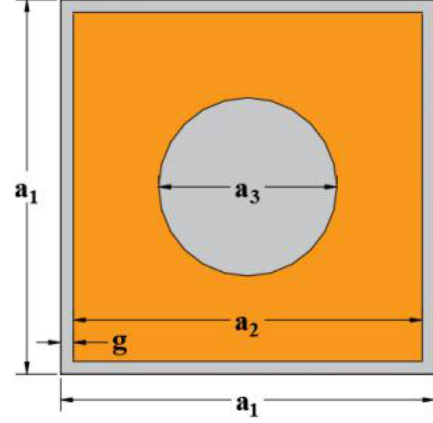


**Figure 4.** EBG structure of the antenna.

antenna. From Figure 3, we can see that the introduced slot structure not only increases the center frequency of the antenna from 2.3 GHz to 2.45 GHz, but also makes the reflection coefficient of the antenna lower and the antenna matching effect better. Table 2 shows the change in bandwidth during antenna evolution.

**Table 2.** The change in bandwidth during antenna evolution.

Antenna	Resonating Frequency	Impedance Bandwidth
Ant1	2.32 GHz	8.2% (2.23–2.42 GHz)
Ant2	2.68 GHz	9.7% (2.56–2.82 GHz)
Ant3	2.30 GHz	14.7% (2.20–2.39 GHz)
Ant4	2.35 GHz	7.7% (2.26–2.44 GHz)
Proposed	2.45 GHz	10.1% (2.34–2.59 GHz)

### 3. DUAL MATERIAL BIONIC FLEXIBLE LOGO ANTENNA BASED ON EBG

#### 3.1. Design of the EBG Structure

A ring-shaped EBG structure is designed to suppress the backward radiation of the antenna. The structure uses polydimethylsiloxane (PDMS) flexible material as the substrate with dielectric constant  $\epsilon_r$  2.65, loss tangential angle  $\tan \delta$  0.02, and the structure is shown in Figure 4. The outer square side length  $a_1$  is 29.4 mm; the inner square copper foil side length  $a_2$  is 28 mm; and the circle diameter  $a_3$  is 14 mm. The thickness  $H$  is 1.5 mm.

The EBG structure units can be regarded as LC resonant circuits, as shown in Figure 5. The annular patch can be equivalent to inductance  $L_1$ .  $C_1$  is the equivalent capacitance between the radiation unit and the ground, and  $C_2$  is the equivalent capacitance between adjacent structural units. The input impedance and resonant frequency of this EBG structure can be calculated from the following formula [13]:

$$Z_0(\omega) = Z_1(\omega) // Z_2(\omega) = \frac{j(1 - \omega^2 C_1 L_1)}{\omega(C_1 C_2 L_1 \omega^2 - C_1 - C_2)} \quad (2)$$

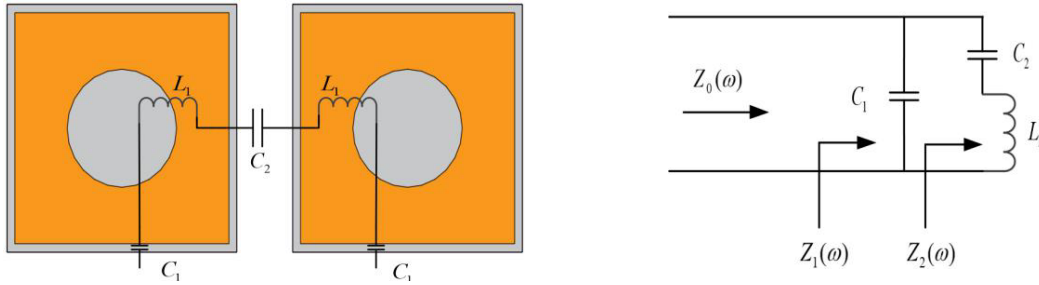


Figure 5. Equivalent circuit between EBG units.

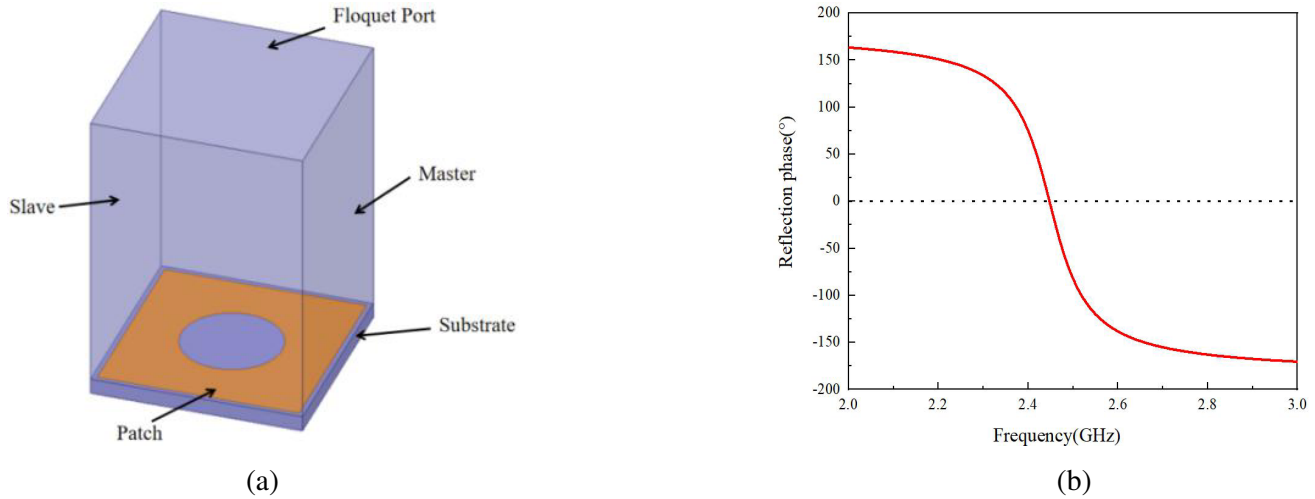


Figure 6. (a) EBG simulation model; (b) EBG structure reflection phase diagram.

$$f_0 = \frac{1}{2\pi} \sqrt{\frac{C_1 + C_2}{C_1 C_2 L_1}} \tag{3}$$

Under normal circumstances, the characteristics of the periodic structure can be verified by a unit, so we only need to use the Floquet port simulation method to establish a simulation model for an EBG unit, as shown in Figure 6(a). By changing the internal structure of the EBG to further adjust the size of the EBG, the final EBG reflection phase diagram is shown in Figure 6(b). It is observed that the zero-phase reflection point of the unit structure corresponds to 2.44 GHz, and the corresponding frequency of the reflection phase interval is 2.37 GHz–2.51 GHz. The reflection phase of EBG is related to many parameters. We select the gap  $g$  between adjacent structural units and the internal circular hole diameter  $a_3$  for parameter analysis, and the simulation results are shown in Figure 7(a). When  $g$  increases from 0.4 mm to 1 mm, the frequency point corresponding to the zero reflection phase moves to high frequency. Through the analysis of the EBG structure, it can be known that when the value of the gap  $g$  increases, the coupling effect between two adjacent units is weakened. The coupling capacitance  $C_2$  also decreases, and from Equation (3), it can be deduced that the resonant frequency  $f_0$  increases. It can be seen from Figure 7(b) that as  $a_3$  increases, the resonant frequency shifts to low frequencies. This is because the increase in the diameter of the circular through hole causes the corresponding equivalent inductance  $L_1$  to increase, so the resonant frequency  $f_0$  decreases.

### 3.2. Dual Material Bionic Flexible Logo Antenna Based on EBG

In order to reduce the impact of antenna radiation on human body, this section proposes the EBG unit loaded under the flexible bionic antenna as shown in Figure 8. The EBG structure uses a  $2 \times 2$  unit array. The distance between the bionic antenna and the EBG structure is very close, and there is

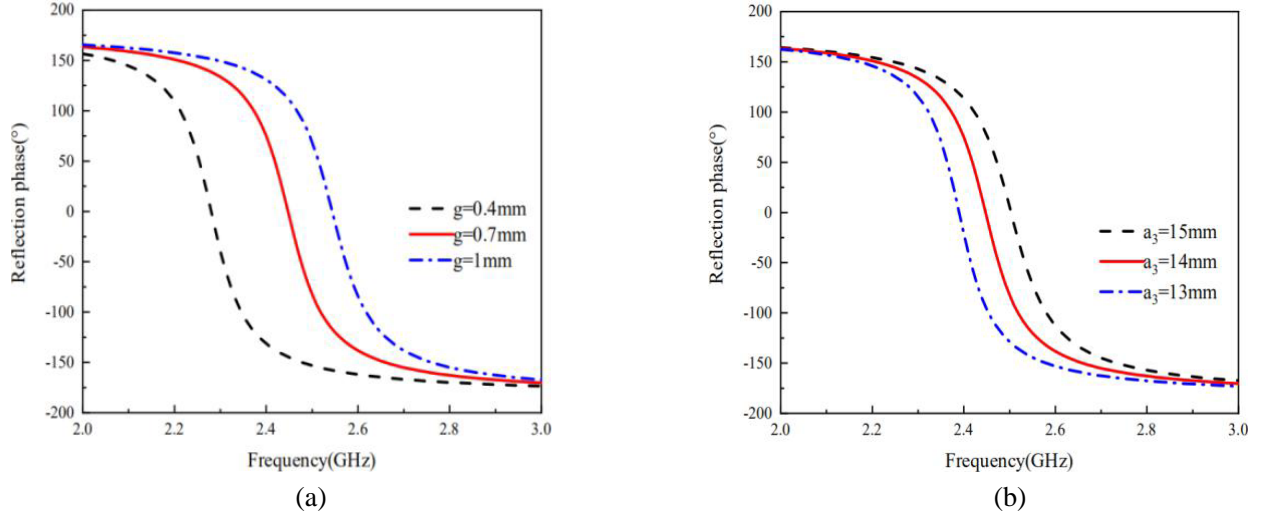


**Figure 7.** The influence curve of the parameter change on the reflection phase. (a) Gap between units  $g$ ; (b) Internal hole diameter  $a_3$ .

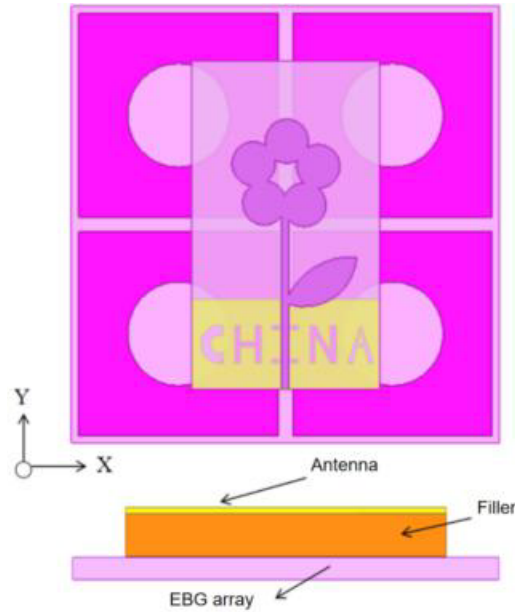


**Figure 8.** Bionic flexible antenna loaded with EBG.

coupling between them, which will affect the impedance matching of the antenna. Therefore, a 2 mm thick foam was added as a filling material between the antenna and the EBG, and the structure is simulated and analyzed.

Figure 9(a) is the prototype of the antenna, and Fig. 9(b) is the prototype of the EBG. The copper sheet is thin and attached to the PDMS using special glue, and the proposed antenna is placed on a foam material to reduce the coupling with the EBG structure. The simulation and measurement results of the antenna, when EBG structure is used and not used, are shown in Figure 10. When the antenna does not adopt an EBG structure, the actual coverage of the antenna is 2.26 GHz–2.65 GHz. Compared with the simulation results, the bandwidth becomes wider, and the value of  $S_{11}$  increases slightly. When the antenna is loaded with the EBG structure, the  $S_{11}$  of the antenna is reduced from  $-25.9$  dB to  $-33.16$  dB, the bandwidth broadened, and the matching effect is better. The measured

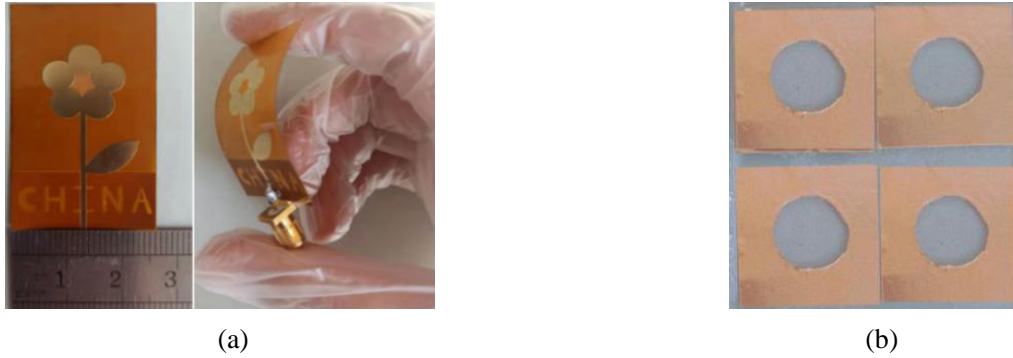


Figure 9. (a) Prototype of the antenna; (b) The prototype of the EBG.

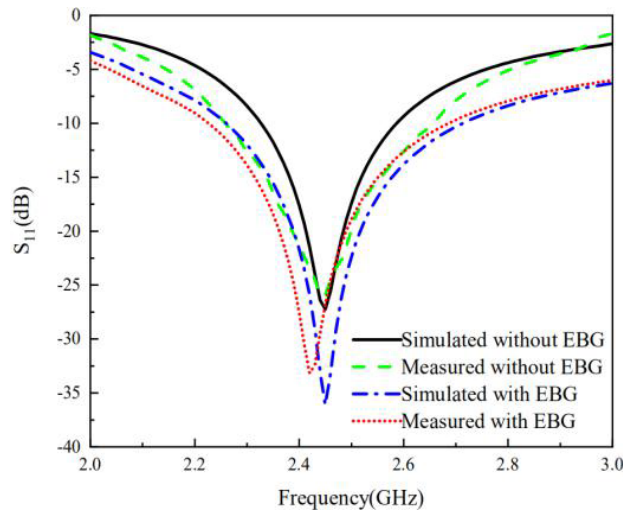


Figure 10.  $S_{11}$  comparison curve before and after loading EBG.

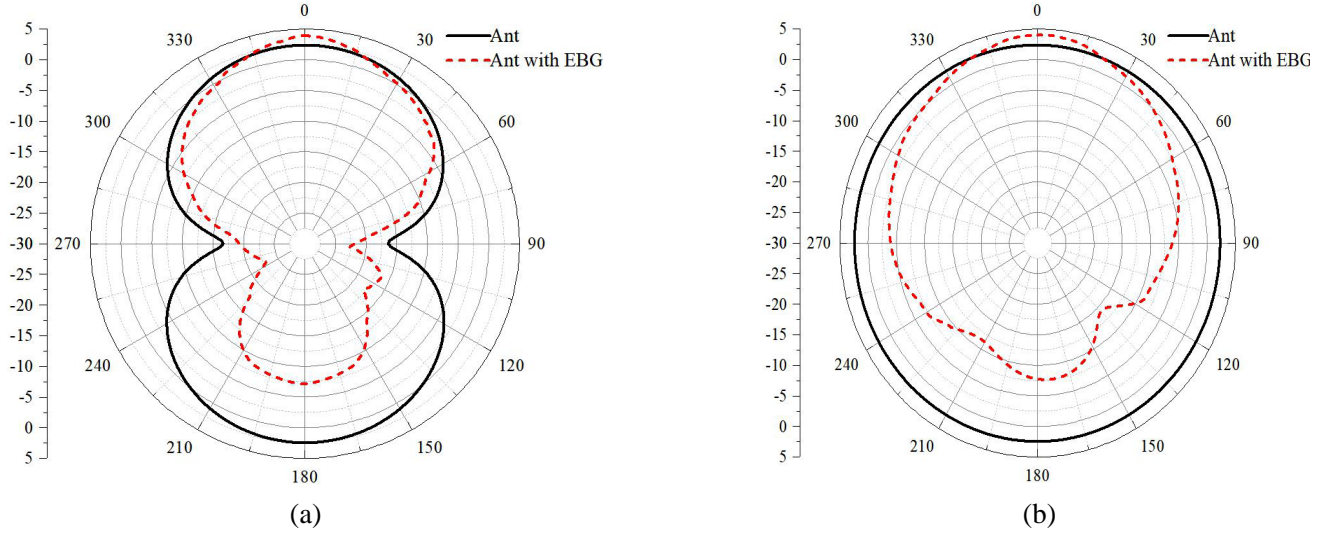
impedance bandwidth of the antenna is 2.22 GHz–2.68 GHz, and the minimum value of  $S_{11}$  is  $-33$  dB.

Figure 11 is the antenna simulation radiation pattern. When the EBG structure is not loaded, the antenna presents omnidirectional characteristics. The back lobe of the antenna is significantly reduced when the EBG structure is loaded, and the main lobe is more concentrated, which increases the front-to-back ratio of the antenna. The EBG structure suppresses the electromagnetic wave of the negative half axis of the  $Z$  axis, and the radiation of the antenna to human body is reduced. In addition, the introduction of this EBG structure can increase the gain from 2.38 dBi to 4.02 dBi.

In terms of structure size, substrate material, bandwidth, and radiation efficiency, the proposed antenna is compared with some related antennas in performance, as shown in Table 3.

Table 3. Comparison of flexible bionic antennas and related antennas.

Ref.	Dimensions (mm)	Dielectric substrate	Impedance bandwidth (GHz)	Gain (dBi)
[1]	50 * 42 * 0.8	FR-4 (Rigid)	3–14 (UWB)	3.95
[3]	127 * 87 * 0.23	Photo paper (Flexible)	2.36–2.61 (10.06%)	0.86
[14]	68 * 38 * 1.57	Rogers RT duroid 5880 (semi Flexible)	2.40–2.50 (4.88%)	6.88
This work	44.2 * 25.9 * 0.2	Polyimide (Flexible)	2.22–2.68 (18.8%)	4.02



**Figure 11.** Radiation patterns of the antenna. (a)  $E$ -plane, (b)  $H$ -plane.

#### 4. EVALUATION OF WEARABLE PERFORMANCE

In traditional monopole antennas, most of the dielectric substrates are made of hard materials, which cannot be bent. The flexible bionic antenna proposed in this paper is made of polyimide, which has good bendability, so it can conform to the human body well. As we know, when the antenna is placed on different parts of human body, such as the front chest, waist, arms, and thighs, the antenna will bend or deform to varying degrees, thereby affecting the performance of the antenna. This section will discuss the effects of different bending directions, different degrees of bending, and different parts of the human body on the performance of the antenna.

##### 4.1. The Effect of Antenna Bending Direction on Antenna Performance

If we put the antenna in different parts of human body, the bending direction will be different. This section discusses the effect of bending on antenna performance when the antenna is bent along the  $x$ -axis and  $y$ -axis. Figure 12(a) shows the simulation model of the bionic pear flower shaped antenna bending along the  $X$  axis, and Figure 13(a) shows the relationship between frequency and reflection coefficient of the antenna under different bending radii. When the bending radius of the antenna decreases, the resonant frequency of the antenna moves to the low frequency, and the value decreases slightly. Through comparison, it can be found that when it is bent 30 mm, 40 mm, and 50 mm along



**Figure 12.** Bionic pear flower shaped antenna structure after bending. (a) Bend along the  $X$  axis; (b) Bend along the  $Y$  axis.

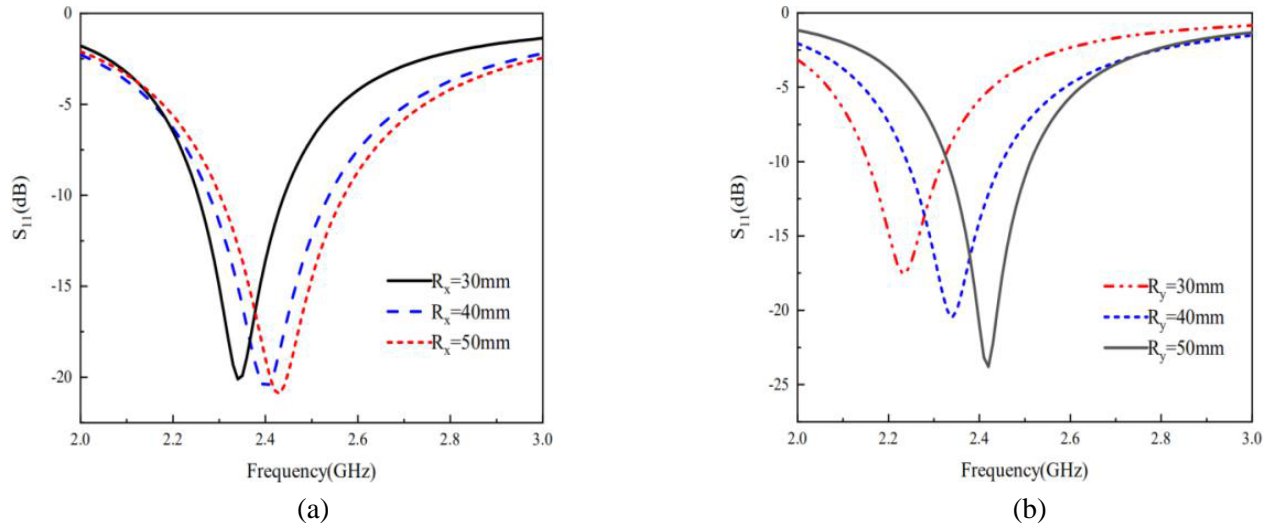


**Figure 13.** Antenna bending performance curve (a) X axis bending; (b) Y axis bending.

the X-axis, the performance of the antenna is lower than that when it is not bent, but the  $-10$  dB impedance bandwidth can still cover the 2.45 GHz operating band.

Figure 12(b) shows the simulation model of the bionic pear flower shaped antenna bending along the Y axis, and the bending circle center is located on the negative half axis of the Z axis. Figure 13(b) shows the comparison of  $S_{11}$  of the antenna with different bending radii. When the antenna bending radius decreases, the value of  $S_{11}$  is continuously increasing. When  $R_y$  becomes 30 mm, the  $S_{11}$  is still below  $-15$  dB, which can still meet the design requirements.

#### 4.2. The Impact of Different Wearing Positions on Antenna Performance

In order to study the influence of different wear positions on antenna performance, we put the antenna on a human body model for simulation. First, simplify the human body into three layers of tissue structure, namely skin, fat, and muscle, and set their thickness to 2 mm, 5 mm, and 20 mm, respectively. Table 4 shows the electromagnetic parameters of human tissue [15]. As shown in Figure 14, the bionic pear flower shaped antenna loaded with EBG structure is placed on the three-layer model of the human body to simulate it. Figure 15 shows the reflection coefficient comparison curve of the bionic pear flower shaped antenna in free space and on human body model. The frequency coverage is 2.3 GHz–2.62 GHz, and the center frequency is 2.44 GHz. Compared with the simulation results in free space, the reflection coefficient is slightly larger, and the antenna bandwidth is narrower.

**Table 4.** Electromagnetic parameters of human tissue.

Human tissue	Dielectric constant	Conductivity (S/m)	Density (kg/m <sup>3</sup> )
Skin	37.95	1.49	1001
Fat	5.27	0.11	900
Muscle	52.67	1.77	1006

The bionic pear flower shaped antenna loaded with an EBG structure is placed at different positions of human body, such as arms and thighs for testing. Figure 16 shows the testing process, and the test results are shown in Figure 17. From Figure 17, we can see the reflection coefficient curve of the antenna on the arm, thigh, and in free space, and the center frequency moves to the low frequency. This is due to the small size of the antenna and the use of flexible dielectric substrate processing. It is difficult for the antenna to maintain a flat state during testing, so there is a certain deviation between the test results

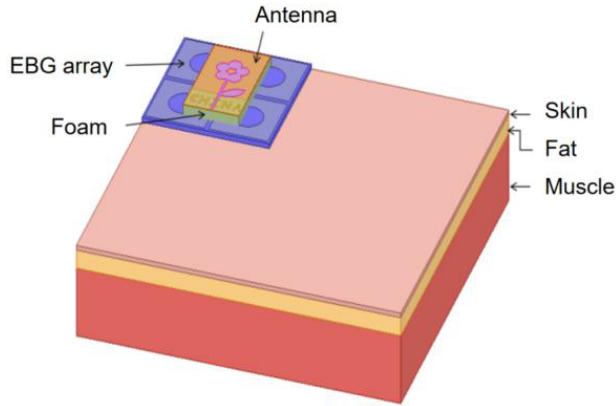


**Figure 14.** The bionic pear antenna is placed on the mannequin.

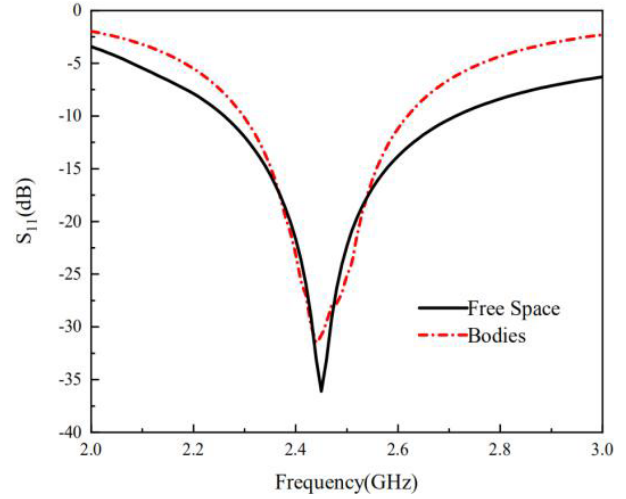


**Figure 15.** Comparison curve of  $S_{11}$  of the antenna in free space and on human body model.



**Figure 16.** Measure on arms and thigh.

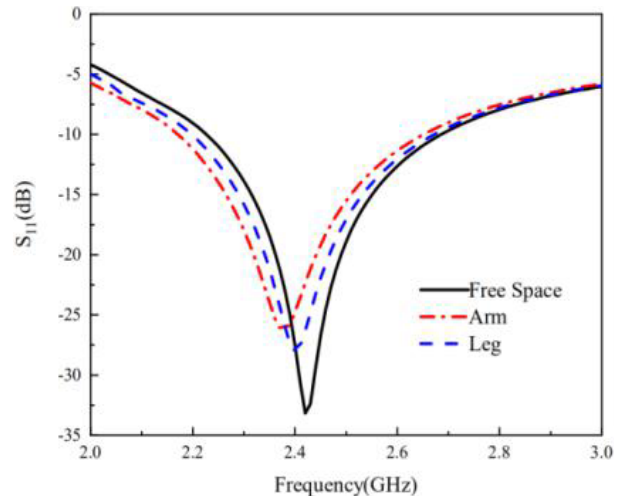


**Figure 17.** Measured comparison  $S_{11}$  curve of antenna in free space, human arm and thigh.

and simulation results. Although the reflection coefficient value varies the most when it is placed on the arm, the performance is still good. The antenna is usually placed on people's arms for easy carrying, and it is recommended that arm is still the preferred wearing position for the proposed antenna.

## 5. CONCLUSION

This paper designs a dual-material bionic pear flower shaped flexible antenna based on an EBG structure. The antenna looks like a pear flower, and a slot is etched on the antenna ground plate to form a "CHINA" logo. The antenna is made of polyimide material. Considering that the antenna will have radiation effect on the human body when people wear it, an EBG structure is introduced to improve the front-to-back ratio of the antenna. PDMS material is chosen for EBG, through the study of its reflection phase, which proves the correctness of the design. The EBG structure was loaded under the flexible bionic pear antenna, and simulation and testing were performed, which met the design requirements. Through the performance simulation of the antenna in bending state and the actual measurement of different human tissues, the rationality of the antenna design is verified.

## ACKNOWLEDGMENT

This work was supported in part by the Research on Key Technologies of accurate positioning of BINGTUAN transportation key vehicles and infrastructure based on Beidou under Grant 2108AB028 and the Project of Young YuYou of North China University of Technology, 2018.

## REFERENCES

1. Jiang, W., Y. Liu, S. Gong, and T. Hong, "Application of bionics in antenna radar cross section reduction," *IEEE Antennas and Wireless Propagation Letters*, Vol. 8, 1275–1278, 2009.
2. Xue, J., Y. Liu, W. Wang, and H. Liu, "A novel broadband bionic Yagi-Uda antenna with low radar cross section," *International Radar Conference, IET*, 2013.
3. Kim, S., Y. J. Ren, H. Lee, A. Rida, S. Nikolaou, and M. M. Tentzeris, "Monopole antenna with inkjet-printed EBG array on paper substrate for wearable applications," *IEEE Antennas and Wireless Propagation Letters*, Vol. 11, 663–666, 2012.
4. Khaleel, H. R., H. M. Al-Rizzo, D. G. Rucker, and S. Mohan, "A compact polyimide-based UWB antenna for flexible electronics," *IEEE Antennas and Wireless Propagation Letters*, Vol. 11, 564–567, 2012.
5. Abbasi, Q. H., M. U. Rehman, X. D. Yang, A. Alomainy, K. Qaraqe, and E. Serpedin, "Ultrawideband band-notched flexible antenna for wearable applications," *IEEE Antennas and Wireless Propagation Letters*, Vol. 12, 1606–1609, 2014.
6. Sundarsingh, E. F., S. Velan, M. Kanagasabai, A. K. Sarma, C. Raviteja, and M. G. N. Alsath, "Polygon-shaped slotted dual-band antenna for wearable applications," *IEEE Antennas and Wireless Propagation Letters*, Vol. 13, 611–614, 2014.
7. Upadhyaya, T., A. Desai, R. Patel, U. Patel, and K. Pandya, "Compact transparent conductive oxide based dual band antenna for wireless applications," *2017 Progress In Electromagnetics Research Symposium — Fall (PIERS — FALL)*, 41–45, Singapore, Nov. 19–22, 2017.
8. A. Desai, C. D. Bui, J. Patel, T. Upadhyaya, G. Byun, and T. K. Nguyen, "Compact wideband four element optically transparent MIMO antenna for mm-Wave 5G applications," *IEEE Access*, Vol. 8, 194206–194217, 2020.
9. Tak, J. and J. Choi, "An all-textile Louis Vuitton logo antenna," *IEEE Antennas and Wireless Propagation Letters*, Vol. 14, 1211–1214, 2015.
10. Monti, G., L. Corchia, and L. Tarricone, "Logo antenna on textile materials," *44th European Microwave Conference (EuMC)*, IEEE, 2014.
11. Rafiee, M. and M. R. Kamarudin, "UTM-logo wideband printed monopole antenna surrounded with circular ring patch," *Progress In Electromagnetics Research C*, Vol. 15, 157–164, 2010.
12. Velan, S., E. F. Sundarsingh, M. Kanagasabai, A. K. Sarma, C. Raviteja, R. Sivasamy, and J. K. Pakkathillam, "Dual-band EBG integrated monopole antenna deploying fractal geometry for wearable applications," *IEEE Antennas and Wireless Propagation Letters*, Vol. 14, No. 1, 249–252, 2015.
13. Liu, X. Y., Y. H. Di, H. Liu, Z. T. Wu, and M. M. Tentzeris, "A planar windmill-like broadband antenna equipped with artificial magnetic conductor for off-body communications," *IEEE Antennas and Wireless Propagation Letters*, Vol. 15, 64–67, 2015.
14. Abbasi, M., S. S. Nikolaou, M. A. Antoniadis, M. Nikolic, and P. Vryonides, "Compact EBG-backed planar monopole for BAN wearable applications," *IEEE Transactions on Antennas and Propagation*, Vol. 65, No. 2, 453–463, 2017.
15. Hu, B., G. Gao, L. He, X. D. Cong, and J. N. Zhao, "Bending and on-arm effects on a wearable antenna for 2.45 GHz body area network," *IEEE Antennas and Wireless Propagation Letters*, Vol. 15, 378–381, 2016.